Published in final edited form as:
Small. 2012 September 24; 8(18): 2904–2912. doi:10.1002/smll.201200873.

A Carbon Nanotube Toxicity Paradigm Driven by Mast Cells and the IL-33/ST2 Axis

Pranita Katwa[†],
Department of Pharmacology & Toxicology, East Carolina University, Greenville, NC 27834, USA

Xiaojia Wang[†],
Department of Pharmacology & Toxicology, East Carolina University, Greenville, NC 27834, USA

Rakhee N. Urankar,
Department of Physiology, East Carolina University, Greenville, NC 27858, USA

Ramakrishna Podila,
Department of Pharmacology & Toxicology, East Carolina University, Greenville, NC 27834, USA

Susana C. Hilderbrand,
Department of Pharmacology & Toxicology, East Carolina University, Greenville, NC 27834, USA

Robert B. Fick,
Division of Biologics, Merck Research Labs, Palo Alto, CA 94304, USA

Apparao M. Rao,
Department of Physics and Astronomy, Clemson University, Clemson, SC 29634, USA

Pu Chun Ke,
Department of Physics and Astronomy, Clemson University, Clemson, SC 29634, USA

Christopher J. Wingard, and
Department of Physiology, East Carolina University, Greenville, NC 27858, USA

Jared M. Brown[*]
Department of Pharmacology & Toxicology, East Carolina University, Greenville, NC 27834, USA

Abstract

Concern about the use of nanomaterials has increased significantly in recent years due to potentially hazardous impacts on human health. Mast cells are critical for innate and adaptive immune responses, often modulating allergic and pathogenic conditions. Mast cells are well known to act in response to danger signals through a variety of receptors and pathways including IL-33 and the IL-1 like receptor ST2. Here, we examined the involvement of mast cells and the IL-33/ST2 axis in the pulmonary and cardiovascular responses to MWCNT exposure. The toxicological effects of MWCNTs were observed only in mice with a sufficient population of mast cells and were not observed when mast cells were absent or incapable of responding to IL-33. Our findings establish for the first time that mast cells and the IL-33/ST2 axis orchestrate adverse pulmonary and cardiovascular responses to an engineered nanomaterial, giving insight into a previously unknown mechanism of toxicity. This novel mechanism of toxicity could be used for

[*]brownja@ecu.edu.
[†]P. Katwa and X. Wang contributed equally to the presented work.

Supporting Information is available on the WWW under http://www.small-journal.com or from the author.

Competing Interests
The authors declare no competing financial interests.

assessing the safety of engineered nanomaterials and provides a realistic therapeutic target for potential nanoparticle induced toxicities.

Keywords

IL-33; ST2; MWCNT; pulmonary fibrosis; myocardial ischemia reperfusion injury; nanotoxicology

1. Introduction

Carbon nanotubes (CNTs) have great versatility in physical and chemical properties leading to increased use in biomedical and technological applications. Their unique properties, including high electrical and thermal conductance, high-strength to weight ratios, and additional novel physico-chemical properties, have led to significantly increased use of CNTs over the past decade.[1, 2] Functionalization of CNTs with amino acids, peptides and other molecules has been an important factor in providing greater stability and lower cellular toxicity compared to non-functionalized or pristine CNTs, making them a promising platform for drug delivery, gene delivery and other biomedical applications.[3–5] While the novel applications of CNTs are advantageous, there is increased concern about their potentially hazardous effects on human health. Despite limited research on direct effects of CNTs on humans, research in animals has demonstrated pristine CNT exposure leads to adverse pulmonary and cardiovascular outcomes. Due to their high aspect ratio characteristics, multi-walled carbon nanotubes (MWCNTs), in particular, have been compared to asbestos fibers and as a result, have been suggested to induce asbestos-like toxicities.[6] Inhalation of MWCNTs in animal models elicits detrimental pulmonary responses including inflammation, granulomatous disease, fibrosis, and altered lung function.[7–10] In addition, MWCNTs exacerbate cardiac ischemia/reperfusion (IR) injury in mice which occurs as early as 1 day post-exposure.[11]

Mast cells are critical for innate and adaptive immune responses, often modulating allergic and pathogenic conditions. Described as key sensors of cell injury, mast cells are well known to act in response to danger signals through a variety of receptors and pathways including pathogen associated molecular pattern (PAMP) receptors, scavenger receptors and the IL-1-like receptor ST2.[12, 13] The ST2 receptor, which can be activated by its ligand interleukin-33, is highly expressed on the surface of mast cells and is pivotal in response to pathogenic and, as suggested, xenobiotic insult.[14]

IL-33, a novel cytokine that is a member of the IL-1 family, has recently been termed an “alarmin” to describe its potential role in alerting the immune system of tissue injury or trauma.[15] Alarmins, also known as endogenous danger signals, have been shown to activate receptors on immune cells in order to initiate inflammatory responses to cell necrosis.[16] IL-33 can induce the release of Th2 pro-inflammatory cytokines, including IL-6 and IL-13 through the ST2 receptor in a variety of immune cells including mast cells.[12, 17, 18] As an alarmin, IL-33 has a dual role in not only initiating immune responses, but modulating them as well.

Our understanding of mast cells in disease has been elucidated through the use of mast cell deficient mice ($Kit^{W\text{-}sh}$ mice). Indeed, $Kit^{W\text{-}sh}$ mice reconstituted with cultured bone marrow derived mast cells (BMMCs) have been utilized as a model for investigating the role of mast cells in numerous conditions.[19, 20] Through the use of this model, our understanding of mast cells now includes their importance in host immune responses to

bacterial infections, airway reactivity in asthma, as well as toxicity of Gila monster and scorpion venoms as examples.[21–23]

In the current study, we examined the contribution of mast cells and the IL-33/ST2 axis to multi-walled carbon nanotube (MWCNT) directed pulmonary and cardiovascular toxicity. As will be shown, MWCNT exposure resulted in adverse pulmonary and cardiovascular responses in mice with sufficient mast cell populations, while these effects were largely absent in mice deficient in mast cells or mice with mast cells unable to respond to IL-33. Our findings establish for the first time that mast cells and the IL-33/ST2 axis modulate adverse pulmonary and cardiovascular responses to an engineered nanomaterial, giving insight into a previously unknown mechanism of toxicity.

2. Results and Discussion

2.1 Mast Cells and the IL-33/ST2 Axis Direct MWCNT Induced Lung Fibrosis

The extent and means by which MWCNTs are able to impact pulmonary toxicity was tested by oropharyngeal aspiration of vehicle or MWCNTs (4 mg/kg) in C57BL/6 mice, $Kit^{W\text{-}sh}$ mice, $Kit^{W\text{-}sh}$ mice reconstituted with BMMCs, $Kit^{W\text{-}sh}$ mice reconstituted with $ST2^{-/-}$ BMMCs and $ST2^{-/-}$ mice. The dose used to elucidate mechanisms of MWCNT toxicity was based upon dose response studies published earlier.[8] In addition, the characteristics of the MWCNTs used in this study have been previously described[8] and are further detailed in Tables 1 & 2 and Supplemental Figure S1. As indicated in Table 2, the MWCNTs were characterized in suspension (10% Infasurf® pulmonary surfactant in saline), which also serves as our vehicle control, and best exemplifies non-agglomerated MWCNTs in a dispersal medium suited for animal studies. Suspension of MWCNTs in surfactants has been shown to increase dispersal and allow for greater stability of the particles, inhibiting aggregate formation and producing greater toxicity.[24] A high zeta potential, as displayed in Table 2, is indicative of a stable suspension, which results in well-dispersed MWCNT.

In distinguishing the specific underlying mechanism(s) of MWCNT induced pulmonary toxicities, we first examined the expression levels of IL-33 in lung tissue. At 30 days post-exposure, all groups of mice exposed to MWCNTs demonstrated a significant increase in IL-33 mRNA levels in lung tissue homogenate compared to vehicle controls (Figure 1a). Protein levels of IL-33 were also significantly elevated in bronchoalveolar lavage fluid (BALF) of C57BL/6 mice 30 days following MWCNT instillation (Figure 1b). Similarly, IL-33 staining of lung tissue sections from MWCNT exposed C57BL/6 mice was notably increased and not co-localized to the nucleus (Figure 1c). Contradictory reports regarding IL-33 function have led to more recent perspectives of IL-33 as a dual-function cytokine; acting as a traditional cytokine and as an intra-nuclear cytokine to regulate gene expression.[25] The extracellular release of IL-33 has also been debated; however, more recent studies demonstrate IL-33 is released by cells following injury and necrosis, unlike apoptotic cells that retain IL-33 intracellularly.[26] Induction of both cellular apoptosis and necrosis can occur with exposure to MWCNTs in cell types such as macrophages and lung epithelial cells.[27, 28] In addition, it has been established that there is an increase in IL-33 expression in lung epithelial cells during inflammation.[29, 30] Therefore, it is possible that our data, displaying increased levels of IL-33 released from lung epithelial cells into the BALF and subsequent mast cell activation, are a result of cytotoxicity due to MWCNT exposure.

Additionally, we conducted *in vitro* studies to confirm the activation of mast cells by IL-33 found within the BALF. It has been reported that IL-33 activation of mast cells occurs independent of the FcεRI pathway.[18] In our study, BMMCs that were treated in culture with BALF collected from C57BL/6 mice instilled with MWCNT display significant

elevation in IL-6 and osteopontin (OPN) mRNA expression compared to BALF from vehicle exposed mice (Figure 2). Increased expression of these two genes was not observed when ST2$^{-/-}$ BMMCs were exposed to BALF from MWCNT instilled mice (Figure 2). These findings validate that the increase in IL-33 found in the lungs of mice treated with MWCNTs is capable of inducing mast cell activation through the ST2 receptor and that IL-33 appears to be the major soluble factor in the BALF capable of mast cell activation.

To further elucidate an IL-33/ST2 axis mechanism in pulmonary inflammation, differential cell counts were obtained from BALF following MWCNT instillation. IL-33 has been identified as a major determinant in the inflammatory processes of the lung.[31] In fact, over expression of IL-33 in transgenic mice demonstrated increased levels of cleaved, mature IL-33, resulting in spontaneous pulmonary inflammation consisting of increased pro-inflammatory cytokines such as IL-5, IL-8 and IL-13, as well as inflammatory cell infiltrates, including neutrophils, in BALF.[32] In our study, differential cell counts at 1 day post-exposure also demonstrated a significantly increased inflammatory cell profile, which is sustained out to 30 days following MWCNT instillation (Supplemental Table S1). At 30 days post-exposure to MWCNTs, C57BL/6 mice and *Kit*$^{W\text{-}sh}$ mast cell deficient mice reconstituted with BMMCs displayed pulmonary inflammation with statistically significant neutrophil recruitment (Figure 3a). The infiltration of neutrophils into the lung was absent in *Kit*$^{W\text{-}sh}$, ST2$^{-/-}$, and *Kit*$^{W\text{-}sh}$ mice reconstituted with ST2$^{-/-}$ BMMCs (Figure 3a). These data therefore suggest the involvement of mast cells, or potentially mast cell derived mediators, in the recruitment of neutrophils. In addition, these data also indicate a role for IL-33 and the ST2 receptor in mediating these responses, as inflammation and neutrophil infiltration is not observed in the absence of ST2 receptors (Figure 3a). Neutrophils have been shown to regulate IL-33 activity through the cleavage of IL-33 into its mature form by neutrophil elastase and Cathepsin G.[33] Neutrophil proteinase 3 (PR3) is also proposed to regulate activity of IL-33 by cleavage into its mature form.[34] While full length IL-33 is biologically active, it has been reported that the activity of mature IL-33 is significantly higher. Furthermore, both the full length and mature forms of IL-33 were detected during neutrophilic infiltration in a murine model of acute lung injury.[33] It is possible that mast cell recruitment of neutrophils along with the capacity of neutrophils in regulating IL-33 activity may impact the inflammatory response induced by MWCNTs. Our data demonstrate a clear role for ST2 receptor mediated mast cell activation in MWCNT induced pulmonary inflammation; however, additional studies may be required to address the potential neutrophil-enhanced IL-33 activity in contributing to these inflammatory responses.

While previous studies have identified pulmonary fibrotic responses induced by MWCNTs, few have examined the underlying mechanisms.[8, 35–37] Studies investigating pro-fibrotic mechanisms, however, have recognized IL-33 as a component in fibrotic responses within the skin, liver and lung.[38–40] Furthermore, it has been reported that mast cells can also mediate fibrotic responses, specifically in response to particulate toxicity as observed with silicosis.[41] Here, we investigated IL-33 in conjunction with its activation of mast cells as an underlying mechanism in MWCNT-specific pulmonary fibrosis. Histopathological changes and collagen deposition, along with quantification of collagen content were examined at 30 days following MWCNT exposure to assess pulmonary fibrotic responses. C57BL/6 mice and *Kit*$^{W\text{-}sh}$ mice reconstituted with BMMCs exhibited a robust increase in collagen content with MWCNT instillation, while *Kit*$^{W\text{-}sh}$, ST2$^{-/-}$, and *Kit*$^{W\text{-}sh}$ mice reconstituted with ST2$^{-/-}$ BMMCs showed a minimal change in collagen content compared to controls (Figure 3b). These data were further substantiated by significantly altered lung histopathology that displayed a wide distribution of collagen deposition and granuloma formation throughout the tissue in C57BL/6 and *Kit*$^{W\text{-}sh}$ mice reconstituted with BMMCs following MWCNT aspiration (Figure 3c). As indicated by Masson's Trichrome staining, fibrotic tissue was identified within granulomas, along with the deposition of MWCNTs as

depicted by arrows (Figure 3c). MWCNT deposition within lung sections was confirmed by Raman spectroscopy (Supplemental Figure S2). In contrast, lung sections from MWCNT instilled *Kit*$^{W\text{-}sh}$ mice did not display any collagen deposition and minimal granulomatous tissue (Fig. 3c). ST2$^{-/-}$ and *Kit*$^{W\text{-}sh}$ mice reconstituted with ST2$^{-/-}$ BMMCs also had an attenuated fibrotic response, suggesting a role for mast cells -- or more specifically -- the ST2 receptor in MWCNT induced pulmonary toxicity.

2.2 MWCNTs Elicit Changes in Pulmonary Function Dependent Upon Mast Cells and IL-33

We have shown that instillation of MWCNTs impairs pulmonary function in C57BL/6 mice due to development of lung inflammation and fibrosis.[8] To investigate whether mast cells and the IL-33/ST2 axis participate in the observed decline in lung function induced by MWCNT exposure, we used the invasive forced oscillation technique to measure elastance (E), compliance (C) and Newtonian resistance (Rn) in C57BL/6 mice, *Kit*$^{w\text{-}sh}$ mice, *Kit*$^{w\text{-}sh}$ mice reconstituted with BMMC, *Kit*$^{w\text{-}sh}$ mice reconstituted with ST2$^{-/-}$ BMMC and ST2$^{-/-}$ mice, 30 days following MWCNT exposure. As previously reported,[8] C57BL/6 mice exhibited a significant increase in E, suggesting increased elastic rigidity of the lungs (Figure 4a). Similarly, *Kit*$^{w\text{-}sh}$ mice reconstituted with BMMCs exhibited significantly increased E following MWCNT exposure, while little or no change in E occurred in *Kit*$^{w\text{-}sh}$ mice, *Kit*$^{w\text{-}sh}$ mice reconstituted with ST2$^{-/-}$ BMMC or ST2$^{-/-}$ mice following MWCNT instillation (Figure 4a). A similar role for mast cells and the IL-33/ST2 pathway was observed when we measured C, which reflects the elasticity of the lung parenchyma and is also influenced by surface tension, smooth muscle contraction and peripheral airway homogeneity. When compared to vehicle treated mice, a reduction in C was observed only in MWCNT instilled C57BL/6 and *Kit*$^{w\text{-}sh}$ mice reconstituted with BMMC (Figure 4b). A decrease in C was not observed when *Kit*$^{w\text{-}sh}$ mice were reconstituted with ST2$^{-/-}$ BMMC or when ST2$^{-/-}$ mice were instilled with MWCNTs. The increased E and the decreased C in C57BL/6 mice and *Kit*$^{w\text{-}sh}$ mice reconstituted with BMMC reveal the increased stiffness in the fibrotic lung due to MWCNT exposure, which is consistent with findings in other models of pulmonary fibrosis.[42] These results indicate that the decline in pulmonary function as a physiological endpoint induced by MWCNT instillation is largely dependent on the presence of mast cells. In addition, our data suggest that the critical mast cell-dependent effects of MWCNT induced pulmonary fibrosis require the ability of mast cells to respond to IL-33 via the ST2 receptor.

A significant increase in Rn following MWCNT exposure was observed in C57BL/6 and *Kit*$^{w\text{-}sh}$ mice reconstituted with BMMC, with little to no change in Rn in *Kit*$^{w\text{-}sh}$ mice, *Kit*$^{w\text{-}sh}$ mice reconstituted with ST2$^{-/-}$ BMMC or ST2$^{-/-}$ mice (Figure 4c). The increased Rn suggests that narrowing of the conducting airways is occurring due to MWCNT exposure. While normal Rn values for mice are around 4.2 $cmH_2O.s/ml$, the *Kit*$^{w\text{-}sh}$ mice in our study displayed abnormally lower values of Rn compared to other groups.[43] However, the lower Rn observed in the *Kit*$^{w\text{-}sh}$ strain was restored to normal values when *Kit*$^{w\text{-}sh}$ mice were reconstituted with C57BL/6 BMMC or ST2$^{-/-}$ BMMC. Studies have shown that *Kit*$^{w\text{-}sh}$ mice reconstituted with BMMCs resulted in notably increased numbers of mast cells in the lung, especially along the central airways, which is similar to the mast cell distribution found in C57BL/6 mice.[44] This suggests that mast cells, which are located along the main bronchi, have a significant impact on Rn. These findings identify an important role for IL-33, and its receptor ST2, in mast cell mediated changes of Rn. Our observations of increases in E and Rn and a decrease in C in C57BL/6 and *Kit*$^{w\text{-}sh}$ mice reconstituted with BMMC but not in *Kit*$^{w\text{-}sh}$ mice, *Kit*$^{w\text{-}sh}$ mice reconstituted with ST2$^{-/-}$ BMMC or ST2$^{-/-}$ mice support the critical role of mast cell activation via IL-33/ST2 axis in MWCNT mediated impairment of pulmonary function.

2.3 MWCNTs Exacerbate Myocardial Ischemia Reperfusion Injury through Mast Cell Activation

Inhalation of ultra-fine, and possibly nano-sized, airborne particulates are well known to elicit adverse cardiovascular events mediated through multiple mechanisms that are largely unclear. We have shown that inhalation of particulates such as cerium oxide nanoparticles can activate mast cells, promoting the release of Th2 pro-inflammatory cytokines and resulting in altered vascular reactivity and exacerbation of an episode of myocardial ischemia/reperfusion injury in C57BL/6 mice, but not $Kit^{W\text{-}sh}$ mice.[45] Additional studies have established that mast cells and/or mast cell products such as chymase are crucial factors in the regulation of cardiovascular responses to tissue injury resulting in inflammation, fibrosis, ventricular arrhythmias and myocardial infarction.[46, 47]

We propose that mast cells are able to contribute to cardiovascular dysfunction, particularly myocardial IR injury, in part, through activation of the ST2 receptor. Clinical observations have reported increased levels of serum soluble ST2 receptor (sST2) associated with decreased left ventricular function and adverse cardiovascular outcomes in patients following acute myocardial infarction.[48] It was therefore of interest to examine how the IL-33/ST2 axis in promoting mast cell activation may potentiate cardiovascular toxicities associated with MWCNT exposure. Work in our laboratory has demonstrated that MWCNT instillation in C57BL/6 mice results in exacerbation of IR injury in a dose dependent manner at 1 day post-exposure, which resolves by 30 days post-exposure.[11] As this cardiovascular response has been shown to occur at an earlier time point, we investigated the role of mast cells and the IL-33/ST2 axis in IR injury responses in mice 1 day following exposure to MWCNTs. Here, we show that instillation of MWCNTs in C57BL/6 mice and $Kit^{W\text{-}sh}$ mice reconstituted with BMMCs exhibit a significant increase in myocardial infarct size following ischemia reperfusion compared to vehicle controls (Figure 5). An exacerbation of the infarct size by MWCNTs was not observed in $Kit^{W\text{-}sh}$ mice or $Kit^{W\text{-}sh}$ mice reconstituted with $ST2^{-/-}$ BMMCs (Figure 5). Interestingly, $ST2^{-/-}$ mice demonstrated a significant exacerbation of infarct size with MWCNT exposure compared to vehicle controls, however, the augmented response was not as robust as seen in C57BL/6 or $Kit^{W\text{-}sh}$ mice reconstituted with BMMCs. These data, while consistent with the pulmonary data in substantiating an underlying mast cell specific mechanism associated with MWCNT toxicity, also suggest that the IL-33/ST2 axis may not solely contribute to mast cell activation which appears to be the major contributing factor in mediating myocardial IR injury responses following MWCNT exposure.

3. Conclusion

In this study, we proposed that MWCNT aspiration actuates the extracellular release of IL-33 in lung tissue, leading to the activation of mast cells through the ST2 receptor, resulting in an increase in pulmonary inflammation, granuloma and fibrotic tissue formation, altered pulmonary function and exacerbated IR injury responses in the heart (Figure 6). We have demonstrated that these MWCNT induced toxicities are mediated by mast cell activation in both the pulmonary and cardiovascular systems, entirely or in part, through the IL-33/ST2 axis. Furthermore, in identifying the mechanism of toxicity, our study provides a crucial insight in delineating efforts to limit exposure to nanoparticles and discerning appropriate means of treatment that could be needed following exposures. There are several possible routes of human exposure to MWCNT. In this study we examined the toxicity of MWCNT through a respiratory exposure route, however, it is important to acknowledge that there is great potential for intravenous exposures as MWCNTs provide a unique platform for drug delivery. Despite the differences in exposure routes, intravenous injection of MWCNTs may result in similar toxicities. Intravenous delivery will distribute MWCNTs into the lung tissue likely leading to similar mast cell mediated pulmonary toxicities as reported in this

study. In addition, as mast cells are known to reside in most tissue types, mast cell driven toxicity should be of concern following intravenous delivery of MWCNTs.[49]

In the current study, we have demonstrated a key role of mast cells as modulators of MWCNT toxicity, therefore, targeting mast cells therapeutically may serve to alleviate the potential toxicities associated with exposure to MWCNTs, and have also provided a novel screening tool to discern the potential toxicity and concern associated with the rising use of nanomaterials.

4. Experimental Section

MWCNT characterization

Multi-walled carbon nanotubes were generously provided by NanoTechLabs, Inc (Yadkinville, NC). The dry powder form of MWCNTs was characterized using transmission and scanning electron microscopy to obtain length, diameter distribution and elemental composition. Raman spectra, surface area, pore volume, pore size distribution, hydrodynamic size, zeta potential and isoelectric point of the MWCNTs were obtained as previously described.[8] A summary of the MWCNT characterization is presented in Tables 1 & 2.

Cell Culture

Bone marrow derived mast cells (BMMCs) were generated from femoral bone marrow of 4 week old female C57BL/6 or $ST2^{-/-}$ mice and grown at 37°C with 5% CO_2. BMMCs and $ST2^{-/-}$ BMMCs were cultured in RPMI 1640 medium supplemented with (10%) FBS, (100μg/mL) streptomycin, (100 U/mL) penicillin, (1 M) sodium pyruvate, non-essential amino acids (Sigma-Aldrich, St. Louis, MO), (25 mM) Hepes, (0.0035%) 2-mercaptoethanol, and (300 μg/mL) recombinant murine IL-3 (Peprotech, Rocky Hill, NJ). FcεRI expression was determined at 4 weeks, at which time >95% of cells were mature BMMCs. In addition, absence of ST2 receptor expression was determined in $ST2^{-/-}$ BMMCs by flow cytometry and IL-33 activation studies. Upon reaching maturity, cells were used for reconstitution of B6.Cg-$kit^{W\text{-}sh}$ mast cell deficient mice or *in vitro* experiments. C57BL/6 or $ST2^{-/-}$ BMMCs used for *in vitro* experiments were exposed to BALF acquired from C57BL/6 mice 1 day post-exposure to MWCNT. C57BL/6 or $ST2^{-/-}$ BMMCs were collected for qPCR analysis of IL-6, IL-33 and OPN, following the 2 hour BALF incubation period.

Experimental Animals

C57BL/6J and B6.Cg-$kit^{W\text{-}sh}$ mast cell deficient mice were acquired from Jackson Laboratories (Bar Harbor, ME, USA) at 4–10 weeks of age. $ST2^{-/-}$ mice were generously provided by Merck, Inc. and breeding colonies were maintained at East Carolina University. In addition, B6.Cg-$kit^{W\text{-}sh}$ mice were reconstituted with wild type (C57BL/6) or $ST2^{-/-}$ BMMCs. They were further divided into 2 treatment groups (6–8 mice/group): vehicle (10% surfactant in saline) or (4 mg/kg) MWCNTs. C57BL/6J, B6.Cg-$kit^{W\text{-}sh}$ (without reconstitution) and $ST2^{-/-}$ mice were also assigned to the same treatment groups. The dose was determined based on previously published a MWCNT dose response data[5]. Mice were lightly anesthetized with isofluorane and received a single dose of MWCNTs (4 mg/kg body weight) or vehicle (10% surfactant) by oropharyngeal aspiration.[21] Clinical grade pulmonary surfactant (Infasurf®) was kindly provided by ONY, Inc (Amherst, NY, USA). Mice were sacrificed at 1 or 30 days post-exposure. Animal protocols and procedures were conducted in accordance with the National Institutes of Health guidelines and approved by the East Carolina University Institutional Animal Care and Use Committee.

Mast Cell Reconstitution of B6.Cg-kit$^{W\text{-}sh}$ Mast Cell Deficient Mice

C57BL/6J and ST2$^{-/-}$ BMMCs were centrifuged at 1200 rpm for 5 min and resuspended in sterile saline. Wild type (C57BL/6J) or ST2$^{-/-}$ BMMCs (5×10^6 cells in 200 μL of sterile saline) were intravenously injected into 4 week old B6.Cg-*kit*$^{W\text{-}sh}$ mice. BMMCs were allowed to reconstitute for 8 weeks at which time reconstituted B6.Cg-*kit*$^{W\text{-}sh}$ mice were instilled with vehicle or MWCNT and sacrificed 1 or 30 days post-exposure for pulmonary and cardiovascular endpoints.

Pulmonary function testing

Elastance (E), compliance (C), and Newtonian resistance (Rn) were measured by forced oscillatory technique using the FlexiVent system (SCIREQ, Montreal, QC, Canada.[8] Briefly, 30 days following instillation of MWCNTs, mice were anesthetized with tribromoethanol (TBE) (400 mg/kg), tracheostomized, and placed on the FlexiVent system. Mice were ventilated with a tidal volume of 10 mL/kg at a frequency of 150 breaths/min and a positive end expiratory pressure of 3 cm H_2O to prevent alveolar collapse. In addition, mice were paralyzed with pancuronium bromide (1 mg/kg) to prevent spontaneous breathing. EKG was monitored for all mice to determine anesthetic depth and potential complications that could have arisen during testing. Total lung capacity (TLC), Snapshot, Quickprime-3, and pressure-volume (PV) loops with constant increasing pressure (PVr-P) were consecutively performed using the Flexivent system. All perturbations were executed until three acceptable measurements with coefficient of determination (COD) ≥ 0.9 were recorded in each individual subject.

BAL and cell differential counts

Following pulmonary function testing, mice underwent *in situ* bronchoalveolar lavage (BAL). The right lung was lavaged four times (26.25 mL/kg body weight) with ice-cold Hanks balanced salt solution (HBSS). Bronchoalveolar lavage fluid (BALF) was collected separately for the first lavage and pooled for the remaining 3 lavages. BALF samples were then centrifuged at 1000 g for 10 min at 4°C and supernatant from the first lavage was snap frozen for cytokine analysis, while cell pellets from all lavage samples were combined and counted, followed by resuspension in (1 mL) HBSS. In order to obtain differential cell counts, 20,000 cells from each BALF sample were centrifuged using a Cytospin IV (Shandon Scientific Ltd., Cheshire, UK) and stained with a three-step hematology stain (Richard Allan Scientific, Kalamazoo, MI, USA). Cell differential counts were determined by morphology with evaluation of 300 cells per slide.

Lung histopathology

Left lungs from mice were perfused with 10% neutral buffered formalin fixative and stored for 24 hrs, then processed and embedded in paraffin. Samples were then sectioned at a thickness of 5 μM and were mounted on slides for staining with hematoxylin and eosin (H&E) or Masson's trichrome stain to detect morphological changes and collagen deposition. MWCNT aggregates localized within the tissue sections were confirmed by Raman spectroscopy.[8]

Immunofluorescence

Unstained histological lung sections from C57BL/6 mice were used for immunofluorescence detection of IL-33. Sections were deparrafinized and subsequently underwent microwave irradiation in citrate buffer for antigen retrieval. Sections were then blocked in (5%) filtered fetal bovine serum in Tris buffer saline (TBS) with (0.2%) Tween and sodium azide for 2 hours, following which IL-33 primary antibody was applied at 1:100 (Novus Biologicals, Littleton, CO) for 48 hours at 4°C. Sections were washed 3 times with TBS and incubated in

a PE (R-phycoerythrin) conjugated secondary antibody at 1:100 (Fitzgerald Industries International, Concord, MA) for 2 hours at room temperature. Following additional washes in TBS with (0.1%) Triton X, sections were coverslipped using Prolong gold anti-fade containing a DAPI stain (Molecular Probes, Eugene, OR). Dry sections were imaged using DAPI and TRITC filters for nuclear and IL-33 specific staining.

Sircol Collagen Assay

Sircol Collagen Assay (Biocolor, Belfast, UK) was used to detect soluble collagen content within the lung homogenate. Lavaged right lung was homogenized in 2 mL of RIPA buffer containing protease inhibitors and the protocol was conducted according to manufacturer's specifications. In addition, a BCA protein quantification analysis was used to determine total protein content for each sample, of which 100 μg of protein used for collagen quantification.

Myocardial Ischemia/Reperfusion (I/R) Injury

At 1 day post-instillation of MWCNT, mice were anesthetized *i.p.* (intraperitoneally) with 0.005 mL/gram body weight of Ketamine/Xylazine mix (18:2 mg/mL) to measure ischemia/reperfusion injury in accordance with an established protocol.[46] In short, following a midline tracheostomy, mice were intubated and ventilated with (100%) oxygen at 115 strokes/min and tidal volume of 0.25 mL, using a Harvard Inspira Ventilator (Harvard Apparatus, Holliston, MA, USA). The pericardium stripped following a thoracotomy to allow for ligation of the left anterior descending coronary artery (LAD). A 06 prolene ligature was used to occlude blood flow for 20 minutes, after which the ligature was released and the myocardium was allowed to reperfuse for 2 hours. The myocardium not subjected to IR injury was determined by infusion of (1%) Evans Blue dye into the aortic arch after which the heart was excised and cut into 1 mm transverse sections. Staining of the sections with 2,3,5-triphenyltetrazolium chloride delineated the area at risk from the infarcted tissue. The area of infarct, expressed as % of area at risk (AAR) was determined Computer Planimetry analysis.

qPCR

Reverse transcription of total lung RNA was performed using a QuantiTect reverse transcription kit (Qiagen). QuantiTect primer assays and SYBR green master mix were utilized for Quantitative real-time PCR to examine mRNA expression levels of IL-33, OPN and IL-6. Cycle threshold (Ct) values and internal reference cDNA levels for the target genes were determined by an Applied Biosystems StepOnePlus Real-Time PCR System (ABI). The cDNA levels were then normalized to GAPDH, used as an internal reference, by the equation $2^{-[\Delta Ct]}$, where ΔCt is defined as Ct_{target}- $Ct_{internal\ reference}$. Values are reported for an average of 4 independent experiments.

ELISA Assays

IL-33 and sST2 levels were measured in BALF using DuoSet ELISA kits (R&D Systems, Minneapolis, MN) in accordance with the manufacturer's instructions. Values are reported as pg/mL.

Statistical Analyses

All data were analyzed by one-way ANOVA, with differences between groups assessed using Bonferroni *post hoc* tests or t-tests and are presented as means ± SEM, where statistically significant differences were identified with $p < 0.05$. All statistical analysis and graphs were generated using GraphPad Prism 5 software (GraphPad, San Diego, CA).

Supplementary Material

Refer to Web version on PubMed Central for supplementary material.

Acknowledgments

This study was funded by NIH RO1 ES019311 (J. Brown), NIH RO1 ES016246 (C. Wingard) and the North Carolina Biotechnology Center (J. Brown). Technical assistance was kindly provided by L. Koehler. In addition, the authors would like to thank Dr. D. Walters for the use of the Flexivent instrument, Drs. B. Harrison and R. Czerw of NanoTechLabs, Inc. for generously providing the multi-walled carbon nanotubes, Dr. W. Kline of ONY Inc. for the generous gift of Infasurf surfactant, and Professor A. Ogale and B. Villa for assistance with the TGA analysis.

References

1. Endo, M.; Strano, M.; Ajayan, P. Potential Applications of Carbon Nanotubes. Vol. Vol. 111. Heidelberg: Springer Berlin; 2008. p. 13
2. The Project on Emerging Nanotechnologies, In.
3. Bianco A, Kostarelos K, Partidos CD, Prato M. Chem Commun (Camb). 2005:571. [PubMed: 15672140]
4. Dumortier H, Lacotte S, Pastorin G, Marega R, Wu W, Bonifazi D, Briand JP, Prato M, Muller S, Bianco A. Nano Letters. 2006; 6:1522. [PubMed: 16834443]
5. Liu Z, Tabakman S, Welsher K, Dai H. Nano Res. 2009; 2:85. [PubMed: 20174481]
6. Poland CA, Duffin R, Kinloch I, Maynard A, Wallace WA, Seaton A, Stone V, Brown S, Macnee W, Donaldson K. Nat Nanotechnol. 2008; 3:423. [PubMed: 18654567]
7. Inoue K, Koike E, Yanagisawa R, Hirano S, Nishikawa M, Takano H. Toxicol Appl Pharmacol. 2009; 237:306. [PubMed: 19371758]
8. Wang X, Katwa P, Podila R, Chen P, Ke PC, Rao AM, Walters DM, Wingard CJ, Brown JM. Part Fibre Toxicol. 2011; 8:24. [PubMed: 21851604]
9. Ryman-Rasmussen JP, Tewksbury EW, Moss OR, Cesta MF, Wong BA, Bonner JC. Am J Respir Cell Mol Biol. 2009; 40:349. [PubMed: 18787175]
10. Huizar I, Malur A, Midgette YA, Kukoly C, Chen P, Ke PC, Podila R, Rao AM, Wingard CJ, Dobbs L, Barna BP, Kavuru MS, Thomassen MJ. Am J Respir Cell Mol Biol. 2011; 45:858. [PubMed: 21398620]
11. Urankar RNLRMME, Katwa P, Wang X, Hilderbrand SC, Harrison BS, Chen P, Ke PC, Rao AM, Podila R, Brown JM, Wingard CJ. In Submission 2012.
12. Enoksson M, Lyberg K, Moller-Westerberg C, Fallon PG, Nilsson G, Lunderius-Andersson C. J Immunol. 2011; 186:2523. [PubMed: 21239713]
13. Abraham SN, St John AL. Nat Rev Immunol. 2010; 10:440. [PubMed: 20498670]
14. Moritz DR, Rodewald HR, Gheyselinck J, Klemenz R. J Immunol. 1998; 161:4866. [PubMed: 9794420]
15. Moussion C, Ortega N, Girard JP. PLoS One. 2008; 3:e3331. [PubMed: 18836528]
16. Kono H, Rock KL. Nat Rev Immunol. 2008; 8:279. [PubMed: 18340345]
17. Moulin D, Donze O, Talabot-Ayer D, Mezin F, Palmer G, Gabay C. Cytokine. 2007; 40:216. [PubMed: 18023358]
18. Ho LH, Ohno T, Oboki K, Kajiwara N, Suto H, Iikura M, Okayama Y, Akira S, Saito H, Galli SJ, Nakae S. J Leukoc Biol. 2007; 82:1481. [PubMed: 17881510]
19. Grimbaldeston MA, Chen CC, Piliponsky AM, Tsai M, Tam SY, Galli SJ. Am J Pathol. 2005; 167:835. [PubMed: 16127161]
20. Wolters PJ, Mallen-St Clair J, Lewis CC, Villalta SA, Baluk P, Erle DJ, Caughey GH. Clin Exp Allergy. 2005; 35:82. [PubMed: 15649271]
21. Sutherland RE, Xu X, Kim SS, Seeley EJ, Caughey GH, Wolters PJ. PLoS One. 2011; 6:e27564. [PubMed: 22110673]

22. Yu M, Tsai M, Tam SY, Jones C, Zehnder J, Galli SJ. J Clin Invest. 2006; 116:1633. [PubMed: 16710480]
23. Akahoshi M, Song CH, Piliponsky AM, Metz M, Guzzetta A, Abrink M, Schlenner SM, Feyerabend TB, Rodewald HR, Pejler G, Tsai M, Galli SJ. J Clin Invest. 2011; 121:4180. [PubMed: 21926462]
24. Wang X, Xia T, Ntim SA, Ji Z, Lin S, Meng H, Chung CH, George S, Zhang H, Wang M, Li N, Yang Y, Castranova V, Mitra S, Bonner JC, Nel AE. ACS Nano. 2011; 5:9772. [PubMed: 22047207]
25. Haraldsen G, Balogh J, Pollheimer J, Sponheim J, Kuchler AM. Trends Immunol. 2009; 30:227. [PubMed: 19359217]
26. Luthi AU, Cullen SP, Mcneela EA, Duriez PJ, Afonina IS, Sheridan C, Brumatti G, Taylor RC, Kersse K, Vandenabeele P, Lavelle EC, Martin SJ. Immunity. 2009; 31:84. [PubMed: 19559631]
27. Di Giorgio ML, Di Bucchianico S, Ragnelli AM, Aimola P, Santucci S, Poma A. Mutat Res. 2011; 722:20. [PubMed: 21382506]
28. Cavallo D, Fanizza C, Ursini CL, Casciardi S, Paba E, Ciervo A, Fresegna AM, Maiello R, Marcelloni AM, Buresti G, Tombolini F, Bellucci S, Iavicoli S. J Appl Toxicol. 2012
29. Talabot-Ayer D, Calo N, Vigne S, Lamacchia C, Gabay C, Palmer G. J Leukoc Biol. 2012; 91:119. [PubMed: 22013230]
30. Pichery M, Mirey E, Mercier P, Lefrancais E, Dujardin A, Ortega N, Girard JP. J Immunol. 2012
31. Yagami A, Orihara K, Morita H, Futamura K, Hashimoto N, Matsumoto K, Saito H, Matsuda A. J Immunol. 2010; 185:5743. [PubMed: 20926795]
32. Zhiguang X, Wei C, Steven R, Wei D, Wei Z, Rong M, Zhanguo L, Lianfeng Z. Immunol Lett. 2010; 131:159. [PubMed: 20412815]
33. Lefrancais E, Roga S, Gautier V, Gonzalez-De-Peredo A, Monsarrat B, Girard JP, Cayrol C. Proc Natl Acad Sci U S A. 2012; 109:1673. [PubMed: 22307629]
34. Bae S, Choi J, Hong J, Jhun H, Hong K, Kang T, Song K, Jeong S, Yum H, Kim S. Endocr Res. 2012; 37:35. [PubMed: 22014109]
35. He X, Young SH, Schwegler-Berry D, Chisholm WP, Fernback JE, Ma Q. Chem Res Toxicol. 2011; 24:2237. [PubMed: 22081859]
36. Mercer RR, Hubbs AF, Scabilloni JF, Wang L, Battelli LA, Friend S, Castranova V, Porter DW. Part Fibre Toxicol. 2011; 8:21. [PubMed: 21781304]
37. Aiso S, Yamazaki K, Umeda Y, Asakura M, Kasai T, Takaya M, Toya T, Koda S, Nagano K, Arito H, Fukushima S. Ind Health. 2010; 48:783. [PubMed: 20616469]
38. Rankin AL, Mumm JB, Murphy E, Turner S, Yu N, Mcclanahan TK, Bourne PA, Pierce RH, Kastelein R, Pflanz S. J Immunol. 2010; 184:1526. [PubMed: 20042577]
39. Marvie P, Lisbonne M, L'helgoualc'h A, Rauch M, Turlin B, Preisser L, Bourd-Boittin K, Theret N, Gascan H, Piquet-Pellorce C, Samson M. J Cell Mol Med. 2010; 14:1726. [PubMed: 19508382]
40. Yanaba K, Yoshizaki A, Asano Y, Kadono T, Sato S. Clin Rheumatol. 2011; 30:825. [PubMed: 21246230]
41. Brown JM, Swindle EJ, Kushnir-Sukhov NM, Holian A, Metcalfe DD. Am J Respir Cell Mol Biol. 2007; 36:43. [PubMed: 16902192]
42. Phillips JE, Peng R, Burns L, Harris P, Garrido R, Tyagi G, Fine JS, Stevenson CS. Pulm Pharmacol Ther.
43. Bates, JHT. Pulmonary mechanics: A system identification perspective; Engineering in Medicine and Biology Society, 2009. EMBC 2009. Annual International Conference of the IEEE; 2009. p. 170
44. Cyphert JM, Kovarova M, Koller BH. Clin Exp Allergy. 2011; 41:260. [PubMed: 20718780]
45. Wingard CJ, Walters DM, Cathey BL, Hilderbrand SC, Katwa P, Lin S, Ke PC, Podila R, Rao A, Lust RM, Brown JM. Nanotoxicology. 2011; 5:531. [PubMed: 21043986]
46. Nistri S, Cinci L, Perna AM, Masini E, Mastroianni R, Bani D. Pharmacol Res. 2008; 57:43. [PubMed: 18068999]

47. Oyamada S, Bianchi C, Takai S, Chu LM, Sellke FW. J Pharmacol Exp Ther. 2011; 339:143. [PubMed: 21795433]

48. Weir RA, Miller AM, Murphy GE, Clements S, Steedman T, Connell JM, Mcinnes IB, Dargie HJ, Mcmurray JJ. J Am Coll Cardiol. 2010; 55:243. [PubMed: 20117403]

49. Yong LC. Exp Toxicol Pathol. 1997; 49:409. [PubMed: 9495641]

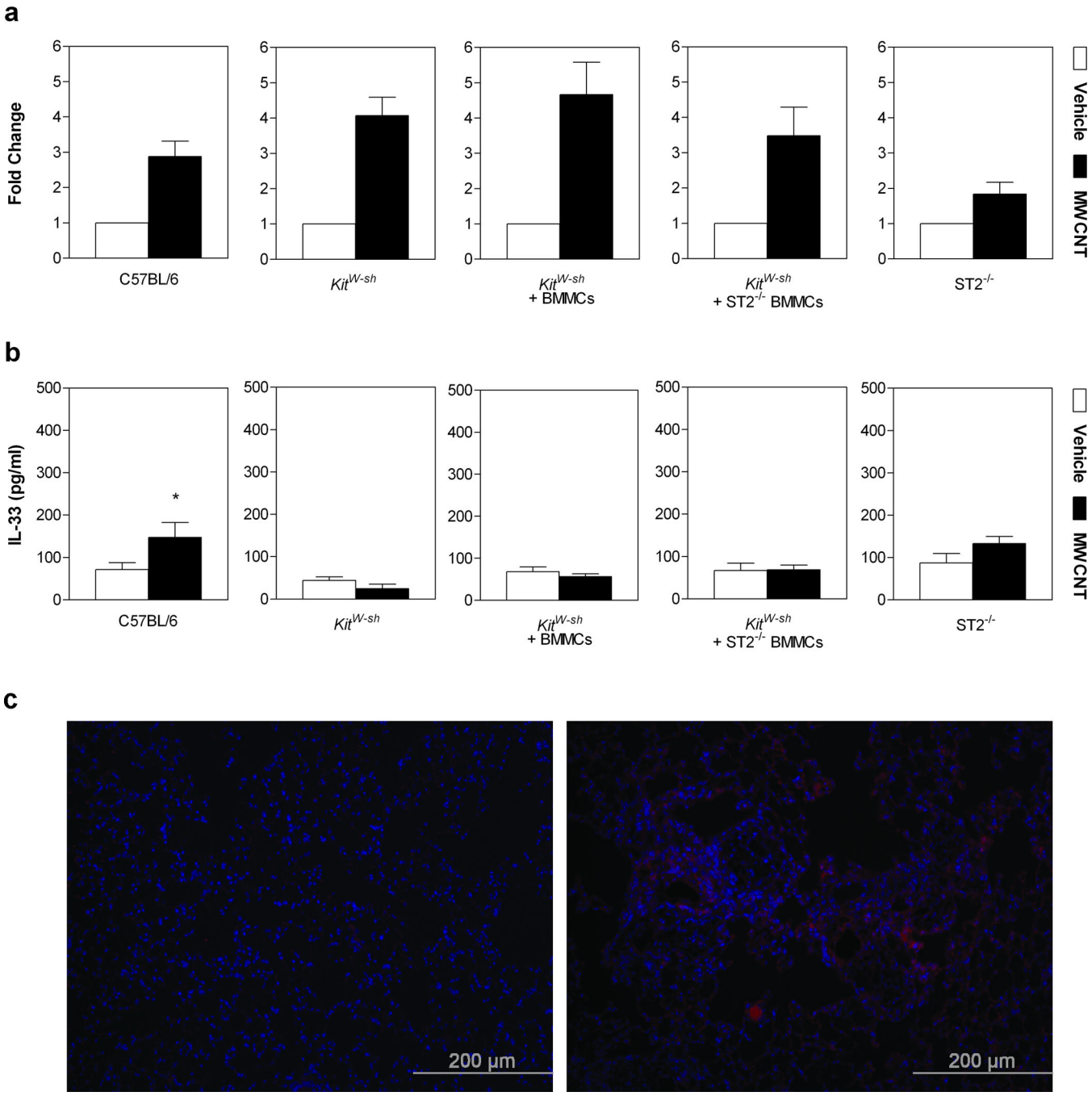

Figure 1. IL-33 Gene and Protein Expression in Lungs of Mice 30 Days Post-Exposure to MWCNT

a, Gene expression of IL-33 in lung tissue, determined by real-time PCR analysis, displayed a >2 fold increase in all groups 30 days post-exposure to MWCNT compared to vehicle controls. **b, c,** Corresponding protein analysis with ELISA **(b)** and immunofluorescence images taken at a magnification of 20× **(c)**. Values are expressed as mean ± SEM (n=6–11). *$p < 0.05$ compared to strain matched vehicle control.

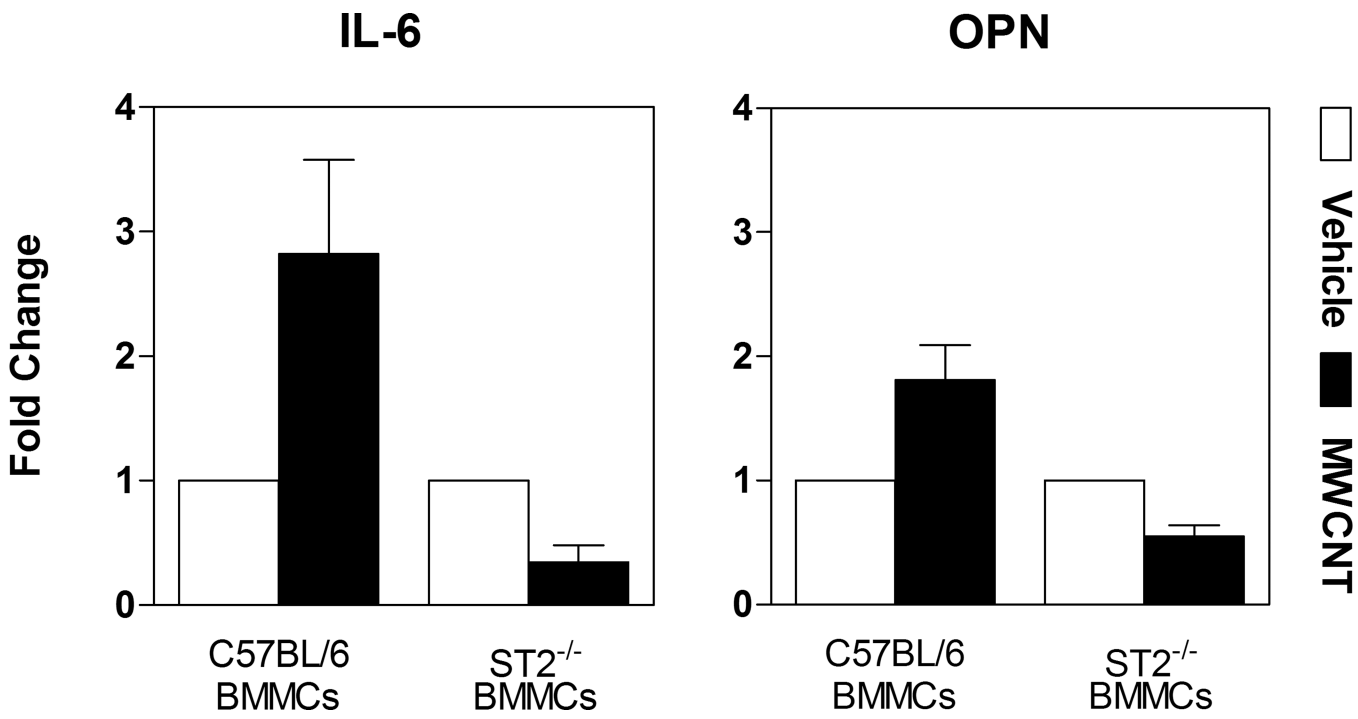

Figure 2. BALF from MWCNT Exposed Mice Results in Mast Cell Activation via the IL-33/ST2 Axis

Gene expression of IL-6 and osteopontin (OPN), determined by real-time PCR analysis, in bone marrow derived mast cells (BMMCs) and $ST2^{-/-}$ BMMCs after 2 hour exposure to bronchoalveolar lavage fluid (BALF) obtained from C57BL/6 1 day following MWCNT instillation. Values are expressed as mean ± SEM (n=3–6).

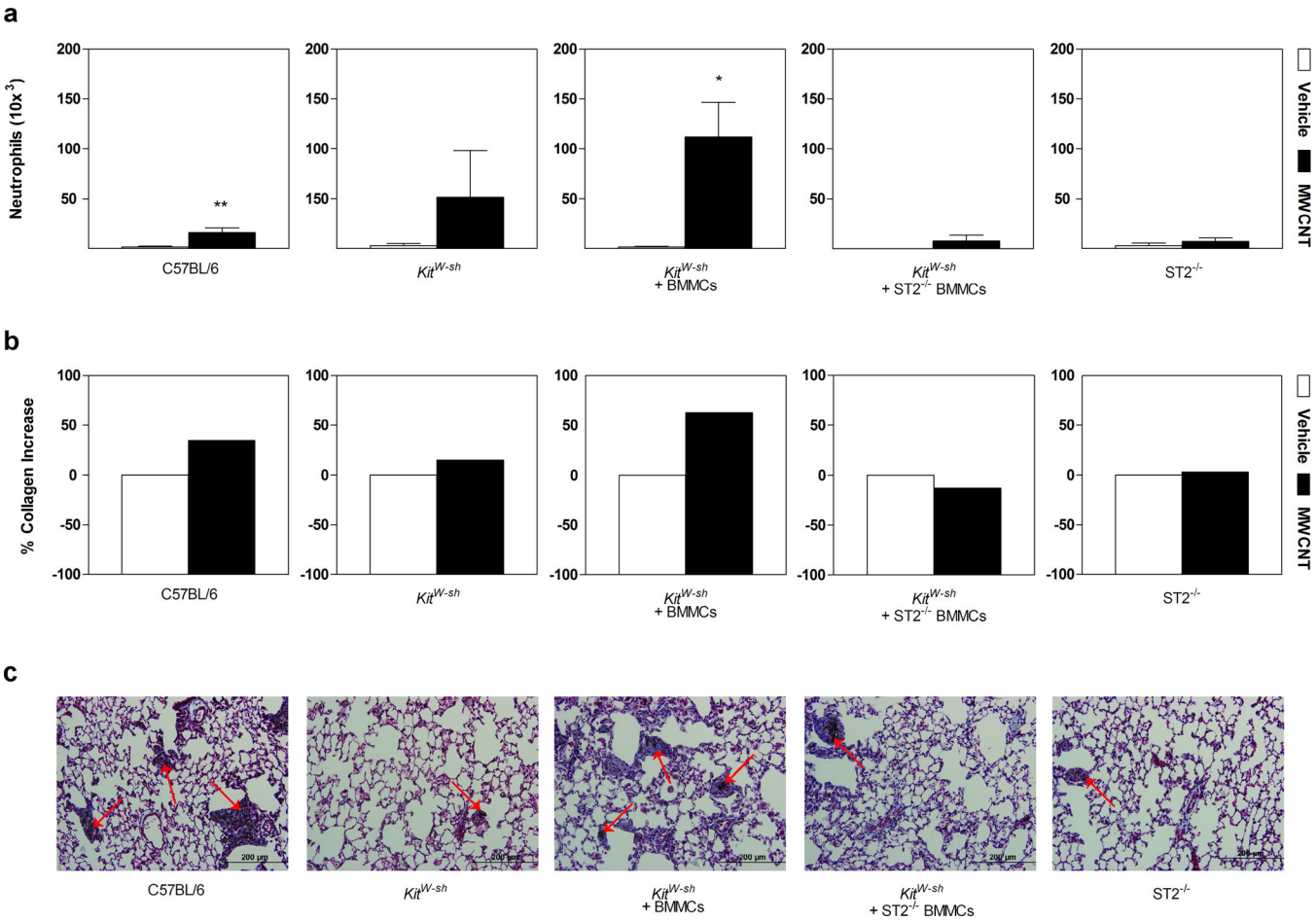

Figure 3. Neutrophil Cell Counts, Histopathology and Collagen Content in Lungs of Mice Instilled with MWCNT

a, Neutrophil cell counts in mice 30 days following instillation with vehicle or MWCNTs. **b**, Percent collagen change in lung tissue of mice exposed to MWCNT at 30 days compared to vehicle control. **c**, Masson's trichrome staining at 30 days post-exposure to MWCNT. As indicated by the bluish color stain, extensive collagen rich granulomas and fibrotic tissue were identified in C57BL/6 and *Kit*$^{W\text{-}sh}$ mice reconstituted with BMMCs. *Kit*$^{W\text{-}sh}$ mice did not display any fibrotic responses, while *Kit*$^{W\text{-}sh}$ mice reconstituted with ST2$^{-/-}$ BMMCs and ST2$^{-/-}$ mice demonstrated minimal granuloma formation, unlike the robust response displayed by mast cell sufficient mice. Agglomerates of MWCNT were identified by Raman spectroscopy[8] and can be seen within granulomas as indicated by arrows. Images are representative of 6–11 mice per group 30 days post-exposure to MWCNT with original magnifications of 20×. All values are expressed as mean ± SEM. *$p < 0.05$ compared to strain matched vehicle control.

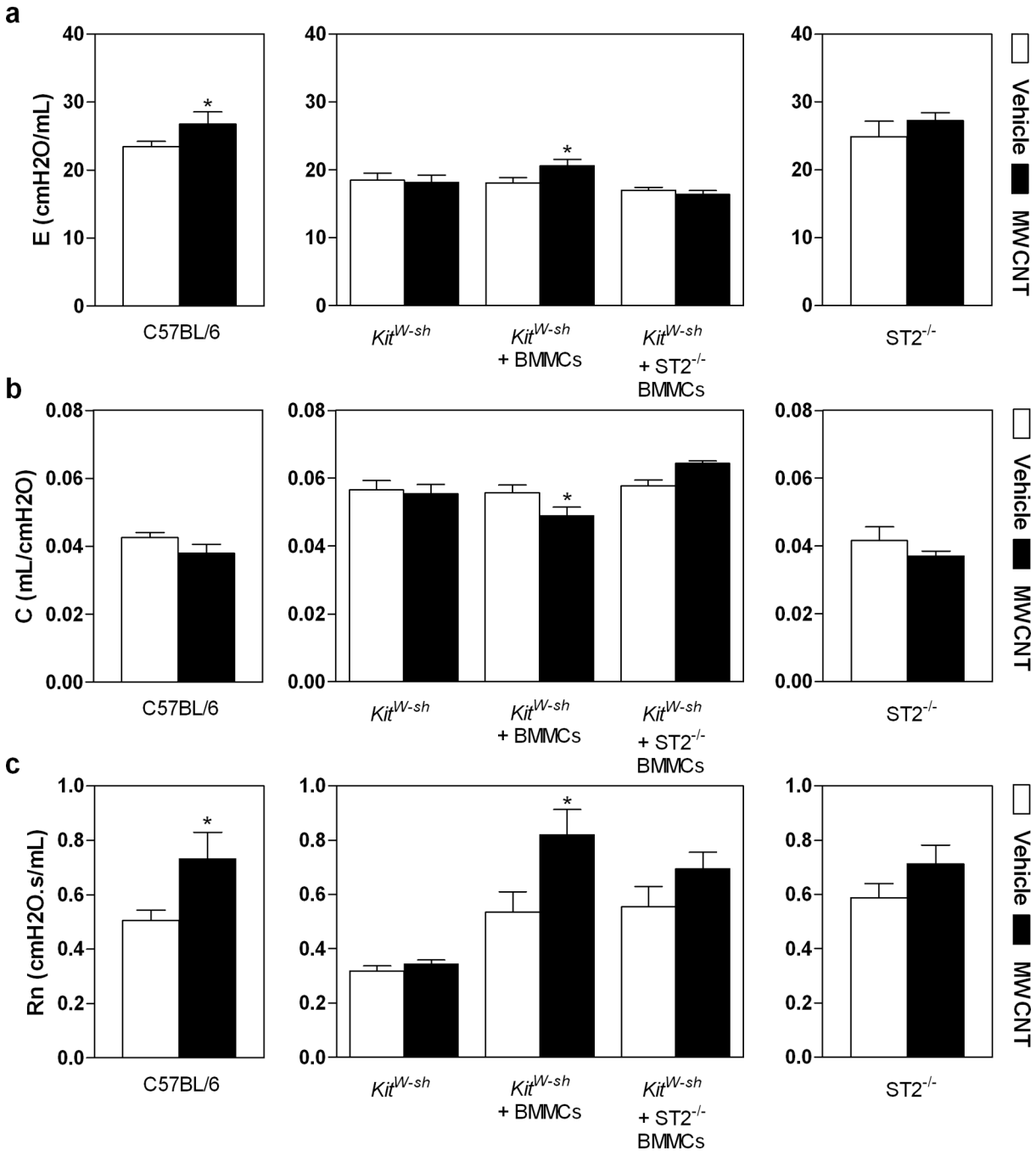

Figure 4. Altered Pulmonary Function Following MWCNT Instillation

The force oscillatory technique was performed on tracheotomized C57BL/6 mice, *Kit*$^{W\text{-}sh}$ mice, *Kit*$^{W\text{-}sh}$ mice reconstituted with BMMC (*Kit*$^{W\text{-}sh}$ + BMMCs), *Kit*$^{W\text{-}sh}$ mice reconstituted with ST2$^{-/-}$ BMMCs (*Kit*$^{W\text{-}sh}$ + ST2$^{-/-}$ BMMCs) and ST2$^{-/-}$ mice 30 days post-instillation with MWCNTs. The perturbation parameters, E (elastance) (**a**), C (compliance) (**b**), and Rn (Newtonian resistance) (**c**) were measured. All values are expressed as mean ± SEM (n=5–6). *$p < 0.05$ compared to strain matched vehicle control (open bar).

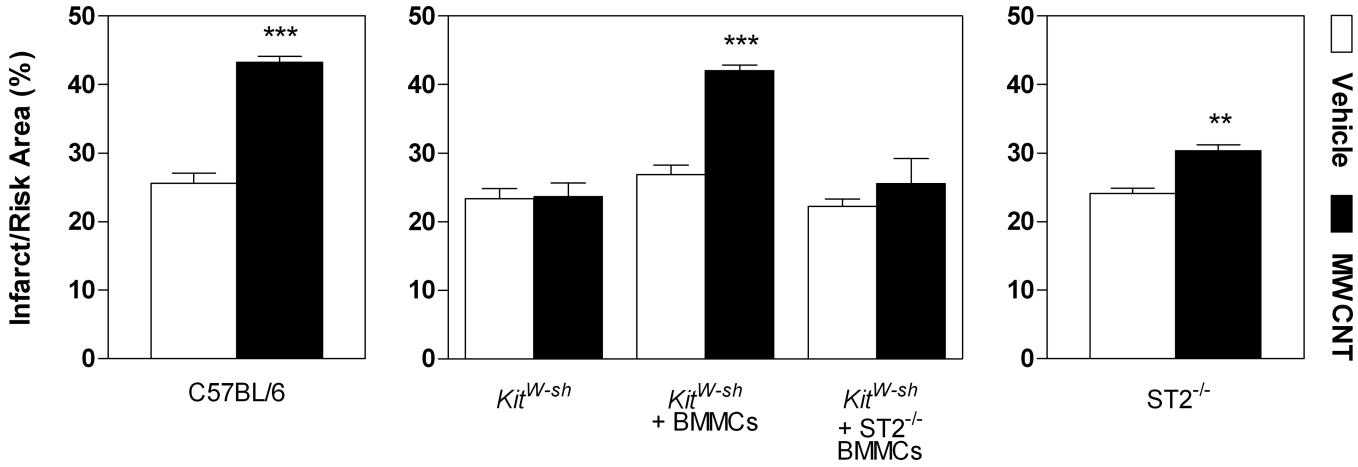

Figure 5. MWCNT Induced Exacerbation of Myocardial Ischemia Reperfusion Injury

Myocardial ischemia reperfusion injury response was assessed as a comparison of infarct size to total area at risk (%) in C57BL/6 mice, *Kit*$^{w\text{-}sh}$ mice *Kit*$^{w\text{-}sh}$ mice reconstituted with BMMCs (*Kit*$^{w\text{-}sh}$ + BMMCs), *Kit*$^{w\text{-}sh}$ mice reconstituted with ST2$^{-/-}$ BMMC (*Kit*$^{w\text{-}sh}$ + ST2$^{-/-}$ BMMCs) and ST2$^{-/-}$ mice, 1 day following exposure to vehicle or MWCNT. All values are expressed as mean ± SEM (n=4–25). $^{**}p < 0.01$ and $^{***}p < 0.001$ compared to strain matched vehicle control.

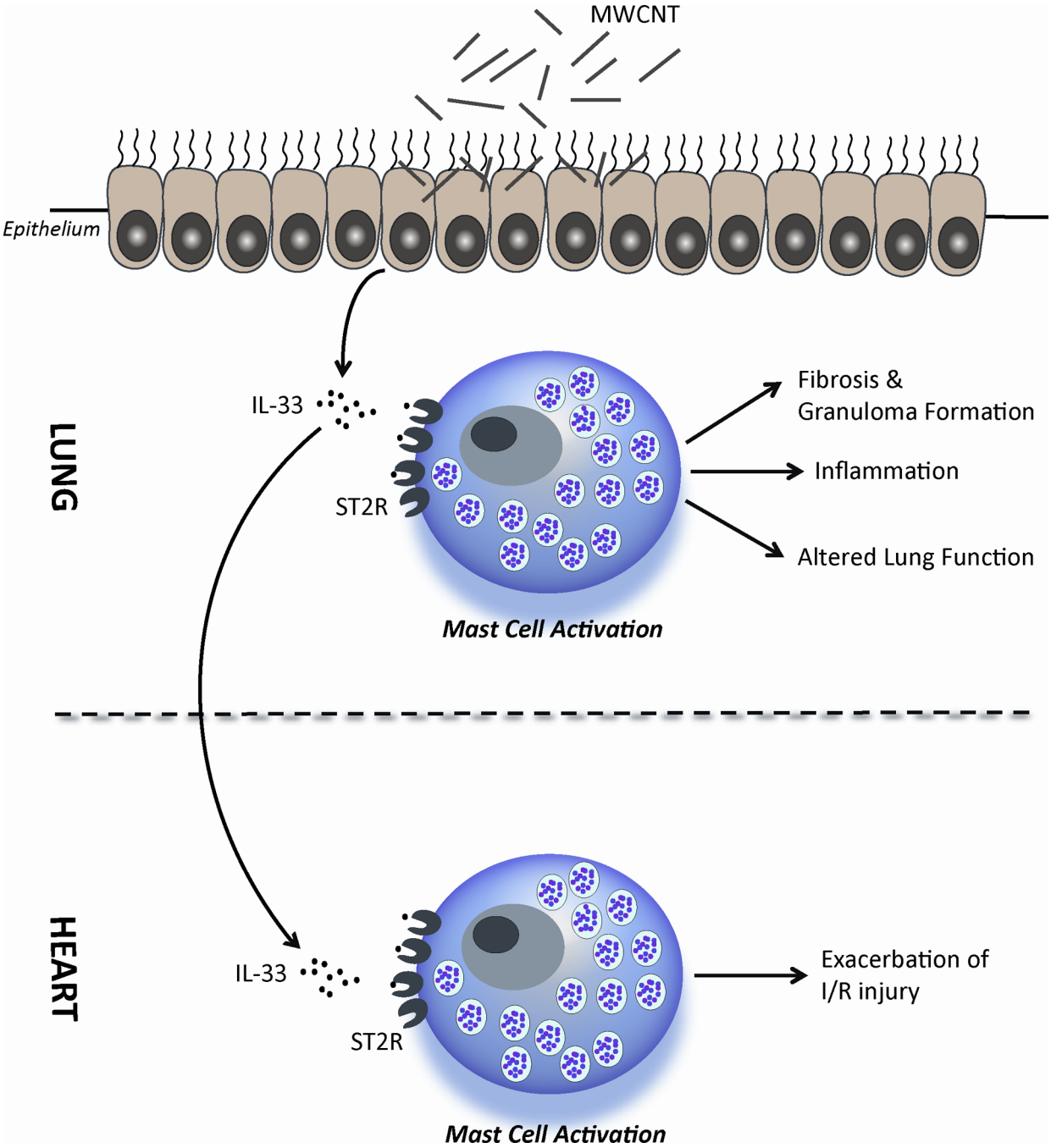

Figure 6. Mechanism of MWCNT Induced Pulmonary and Cardiovascular Toxicity

MWCNT induced injury to the lung epithelium results in the release of IL-33. In the lung, IL-33 can activate mast cells through the ST2 receptor to induce pulmonary inflammation, granuloma formation and fibrosis, as well as altered lung function. A similar mechanism in the heart may influence the activation of mast cells by IL-33 via ST2 receptors to exacerbate ischemia reperfusion injury responses.

Table 1

MWCNT Characteristics

	Mean Diameter by TEM (nm)	Length Range by TEM (μm)	Metal Ash Content by TGA (% weight)	Spectral Content (Atomic %)		Surface area by BET (m^2/g)	Pore volume by BJH (cm^3/g)
				C	Fe		
MWCNT	22.5 ± 1.3	10 – 100	4.80	99.6	0.04	113.10	0.69

Table 2

MWCNT Suspension Characteristics

			Hydrodynamic Size	
	Zeta Potential	**IEP**	**Major peak**	**Minor peak**
MWCNT	− 44.6 mV	pH = 3.5	180 ± 50 nm	1100 ± 200 nm